Available online at www.sciencedirect.com
SCIENCE DIRECT®
Pergamon
Cement and Concrete Research 34 (2004) 1121–1130
CEMENT AND CONCRETE RESEARCH

Shrinkage cracking of lightweight concrete made with cold-bonded fly ash aggregates

Mehmet Gesoğlu, Turan Özturan*, Erhan Güneyisi

Department of Civil Engineering, Boğaziçi University, Bebek, Istanbul 34342, Turkey

Received 28 July 2003; accepted 26 November 2003

Abstract

Shrinkage cracking performance of lightweight concrete (LWC) has been investigated experimentally on ring-type specimens. LWCs with and without silica fume were produced at water–cementitious material ratios (w/cm) of 0.32 to 0.55 with cold-bonded fly ash coarse aggregates and natural sand. Coarse aggregate volume ratios were 30%, 45%, and 60% of the total aggregate volume in the mixtures. A total of 12 lightweight aggregate concrete mixtures was cast and tested for compressive strength, static elastic modulus, split-tensile strength, free shrinkage, weight loss, creep, and restrained shrinkage. It was found that the crack opening on ring specimens was wider than 2 mm for all concretes. Free shrinkage, weight loss, and maximum crack width increased, while compressive and split-tensile strengths, static elastic modulus, and specific creep decreased with increasing coarse aggregate content. The use of silica fume improved the mechanical properties but negatively affected the shrinkage performance of LWCs. Shrinkage cracking performance of LWCs was significantly poorer than normal weight concrete (NWC).

Keywords: Creep; Lightweight concrete; Mechanical properties; Silica fume; Shrinkage

1. Introduction

Lightweight aggregate concrete has been used successfully for structural purposes for many years. They are naturally utilized in structures for which major part of the total load is due to the dead weight of concrete. Commercially available lightweight aggregates, such as expanded clay or shale, and sintered fly ash, are obtained through heat treatment at 1000 to 1200 °C [1]. An alternative way of producing lightweight aggregate with an environmental impact and minimum energy consumption is the agglomeration of fly ash particles by cold-bonding process, where the water is the wetting agent acting as coagulant, so that the moist mixture would be pelletized in a tilted revolving pan. Lime or Portland cement is used as binder. By using such aggregates, it has been possible to produce structural lightweight concrete (LWC) with 28-day compressive strength up to 30 MPa [2,3].

LWCs have certain properties that are distinctly different from normal weight concrete (NWC). In addition to low unit weight, better reinforcing steel–concrete bond, durability performance, tensile strain capacity, and fatigue resistance make it preferable to NWC [4–6]. However, the wide diversity of the lightweight aggregate source and manufacturing process result in distinctive behavior among the LWCs. Therefore, properties of LWCs should be investigated independently for each type of lightweight aggregate [7].

LWC mixes are generally of low water–binder ratio (w/b) to compensate the aggregate weakness. Apart from the higher amount of cementitious material in the concrete mix, lower modulus of elasticity of the aggregate make the shrinkage of LWC very crucial. Neville [8] indicated that lightweight aggregate results in higher shrinkage values than normal weight aggregate. Nielsen and Aitcin [9] investigated the drying shrinkage of LWC incorporating expanded shale. Different from Neville [9], they found that LWC had 30% to 50% lower shrinkage than the companion NWC after 28 days of curing and 56 days of drying. They attributed this to the presence of water inside the aggregate particles. Likewise, Newman [10] stated that LWC with dense fine aggregates exhibited similar shrinkage perfor-

* Corresponding author. Tel.: +90-212-3581540x1450; fax: +90-212-2872457.
E-mail address: ozturan@boun.edu.tr (T. Özturan).

0008-8846/$ – see front matter © 2003 Elsevier Ltd. All rights reserved.
doi:10.1016/j.cemconres.2003.11.024

mance as NWC and that the shrinkage cracking was rare in LWC due to the relief of restraint by creep and the continuous supply of moisture from the pores of the lightweight aggregate. Another research was conducted by Kayali et al. [7] on LWCs made of Lytag aggregates (sintered fly ash) with a total cementitious material content of 785 kg/m^3. This study [7] revealed that the drying shrinkage (about 1000 microstrain) was nearly twice that of NWC after 400 days, where the NWC had a cementitious material content of 485 kg/m^3. To reduce shrinkage, steel or polypropylene fibers were added into the fresh concrete. However, reinforcing the concrete with fibers did not seem to impart any benefit other than reducing the drying shrinkage. Shrinkage performance of Lytag aggregate was also investigated by Al-Khaiyat and Hague [11]. After 6 days of curing of demoulded specimens, they were exposed to long-term drying. Drying shrinkage was 640 microstrain, which was moderately high, at the age of 3 months. It is strongly evident that various types of lightweight aggregate usually result in very different behavior as far as drying shrinkage is concerned.

The research mentioned above were all based on the drying shrinkage measured on free specimens cured for at least 7 days. They have usually overlooked the shrinkage performance at an early age despite the fact that early age deterioration of concrete is a persistent problem that arises especially from autogenous and/or drying shrinkage [12]. Moreover, free shrinkage tests may not offer sufficient information on the behavior of concrete structures inasmuch as virtually all concrete elements are restrained in some way [13]. Concrete will be expected to crack whenever the induced tensile stress exceeds its tensile strength. Tensile strength of concrete is initially zero and increases with time. The effect of thermal strain resulting from the heat of hydration may be additive with shrinkage strain. For a given level of strain, higher material stiffness will lead to higher tensile stress. Creep, usually considered an undesirable property of concrete, on the other hand, acts as a mechanism of stress relief, reducing tensile stress.

Several studies on shrinkage cracking of NWC are reported in the literature [12–18]. Test methods commonly used for measuring shrinkage cracking of concrete are bar test, plate test, ring test, and some recently developed techniques [12,14]. The new methods include a layer of fresh concrete placed directly on a hardened rough substrate, and restrained and unrestrained tests of dog-bone specimens. The bar test has several disadvantages in providing constant restraint. The plate test provides a biaxial restraint that depends on geometry and boundary conditions. The ring test provides a high and nearly constant restraint. Because of the axysymetry, the geometry and the boundaries do not significantly influence the result. Inasmuch as the free shrinkage of the bar and that of the ring specimen have been shown to be equal, this test method has considerable promise [13,15]. Table 1 shows the restrained shrinkage test results from the literature obtained through the ring specimens of NWC at different strength levels.

Table 1
Restrained shrinkage test data for NWC on ring specimens as reported in literature

Reference no.	Curing time (h)	Compressive strength (MPa)	Drying period (days)	Final shrinkage (microstrain)	Crack width (mm)	Cracking age (days)
15	2.5	24	7	–	0.175	–
15	96	24	42	1025	0.900	6
16	4	36	42	540	0.720	6
18	96	–	42	900	0.530	–
17	5	33	42	650	0.980	10
13	6	53	90	640	0.550	10
13	6	67	90	770	0.600	10
13	6	74	90	770	0.750	8
13	6	85	90	810	0.950	6

The main objective of this paper is to investigate the shrinkage cracking of lightweight aggregate concrete made with cold-bonded fly ash aggregates. In addition to the restrained and free shrinkage performance of the drying specimens, creep, compressive and splitting tensile strengths, and static elastic modulus of concrete were experimentally investigated. Concrete mixtures with and without silica fume at water–cementitious material ratios (w/cm) varying from 0.32 to 0.55 were cast with coarse aggregate volume concentrations of 30%, 45%, and 60% of the total aggregate content. An addition of 10% silica fume by weight of cement was used to investigate the effect of silica fume on the abovementioned properties of the LWC, considering the change in w/cm of the mixtures.

2. Experimental details

2.1. Aggregates

Cold-bonded fly ash lightweight coarse aggregates were used in the concrete production. A dry powder mixture of 90% fly ash and 10% ASTM Type I Portland cement by weight was pelletized through moistening in a revolving tilted pan at ambient temperature. Properties of the fly ash and the cement are shown in Table 2. During the first 10 min of the agglomeration process, water was sprayed onto the fly ash–portland cement powder mixture to act as coagulant in the pelletization process. Agglomeration was continued for an additional 10 min for further stiffening of the fresh pellets. Then, the fresh pellets were put in sealed plastic bags and were stored for the hardening in a curing room at a temperature of 20 °C and 70% relative humidity for 28 days. At the end of the curing period, aggregates were sieved, and only those passing a 9.5-mm sieve and were retained on a 4-mm sieve were selected as the coarse aggregate. Specific gravity of the SSD aggregates was 1.78, and water absorption at 24 h was 24% by weight. Relatively high specific gravity of the fly ash caused a slight

Table 2
Chemical and physical properties of cement, fly ash, and silica fume

Analysis report		Cement	Fly ash	Silica fume
SiO_2 (%)		20.1	36.9	85.8
Al_2O_3 (%)		4.1	17.2	1.1
Fe_2O_3 (%)		4.3	4.8	0.9
CaO (%)		63.4	33.2	1.9
MgO (%)		1.2	1.4	2.6
SO_3 (%)		2.4	3.8	1.0
Na_2O (%)		–	0.3	0.3
K_2O (%)		–	1.8	4.1
Insoluble residue (%)		0.4		0
Loss of ignition (%)		2.6	0.2	1.8
Free lime (%)		1.5	–	–
C_3S (%)		58.9	–	–
C_2S (%)		13.1	–	–
C_3A (%)		3.6	–	–
C_4AF (%)		13.2	–	–
Specific weight		3.1	2.6	2.3
Vicat start/stop (hr:min)		184/229	–	–
Le Chatelier (mm)		3	–	–
Fineness (%)	45 mm	11	23.3	27.7
	90 mm	0.3	9.9	4.5
	200 mm	–	2.7	1.2
Specific surface area (cm^2/g)		3499	3206	20500

increase in that of the aggregates compared to various other artificial lightweight aggregates [1–3]. Natural sand of two size groups, 0–1 and 0–4 mm, was used as fine aggregate. Specific gravity of the sand was 2.60.

2.2. Mix proportioning and casting of concrete

LWC specimens were cast using ASTM Type I Portland cement, lightweight fly ash coarse aggregate, natural sand, water, superplasticizer, and condensed silica fume in some cases. Properties of silica fume are given in Table 2. A total of 12 concrete mixtures was produced at low (0.32 and 0.35) and high (0.50 and 0.55) w/cm. Cement content was 550 and 400 kg/m^3 for low and high w/cm ratio mixtures, respectively. The mixtures for each w/cm were prepared with lightweight coarse aggregate covering 30%, 45%, and 60% by volume of the total aggregate in the mixture, and the remaining 70%, 55%, and 40% of the total aggregate volume were occupied by natural sand fine aggregate. Actual proportions for 1-m^3 concrete are given in Table 3.

A special procedure was followed for batching, mixing, and casting of concrete to minimize the early slump loss due to the high water absorption of lightweight aggregates. Concrete mixtures were designed to have a 200 ± 20-mm slump, which was realized by using a superplasticizer. Lightweight fly ash aggregates were first immersed in water for 30 min for saturation and then laid on a lower sized sieve for an additional 30 min for the seepage of excessive surface water. Concrete was mixed in a laboratory pan mixer. First, the saturated-surface-dry lightweight aggregate was mixed with the Portland cement and the silica fume if used. Then, the natural sand was added into the mixer. Finally, the water containing the superplasticizer was added gradually to this mixture, which was continued to be mixed for about 4 min. Slump and density were then measured. After that, the concrete mixture was poured into the steel moulds in two layers, each of which being vibrated for a couple of seconds.

2.3. Test specimens

Specimens were cast from a typical mixture consisted of three 100 mm-cubes for compressive strength testing, three 100×200-mm cylinders for splitting tensile strength and modulus of elasticity determination, four $50 \times 50 \times 300$-mm prisms to monitor the free shrinkage and weight loss, two ring specimens to monitor the restrained shrinkage cracking, and two $75 \times 75 \times 300$-mm prisms for creep tests.

Ring-type specimens were used in this study to observe the restrained shrinkage-induced cracking of concrete. The scheme and the dimensions of the ring mould and the photograph of a cracked specimen (M6) are shown in Figs. 1 and 2, respectively. For such a ring, as the concrete was subjected to an internal pressure induced by the restraining inner steel tube, the difference between the values of the tensile hoop stress on the outer and the inner surface of the concrete was only 10%. Also, the maximum value of the

Table 3
Actual mix proportions for 1 m^3 concrete (in kg/m^3)

Mix no.	w/c	w/cm	Cement	Water	Silica fume	HRWRA[a]	LW Aggregate	Natural sand	Crushed sand	Fresh density
M1	0.35	0.35	547.3	191.6	–	15.6	323.0	764.7	327.7	2170
M2			549.5	192.3	–	11.0	486.5	603.2	258.5	2101
M3			547.4	191.6	–	5.5	646.2	437.1	187.3	2015
M4		0.32	545.0	190.7	54.5	16.1	307.8	728.7	312.3	2155
M5			546.0	191.1	54.6	11.5	462.5	573.6	245.8	2085
M6			549.0	192.2	54.9	9.4	620.2	419.5	179.8	2025
M7	0.55	0.55	396.1	217.8	–	6.9	336.4	796.4	341.3	2095
M8			399.4	219.7	–	2.5	508.9	631.0	270.4	2032
M9			400.8	220.4	–	0.0	680.8	460.5	197.4	1960
M10		0.50	396.2	217.9	39.6	8.9	326.4	772.8	331.2	2093
M11			398.6	219.2	39.9	3.0	492.6	610.9	261.8	2026
M12			398.6	219.2	39.9	1.0	656.8	444.2	190.4	1950

[a] High-range water-reducing admixture.

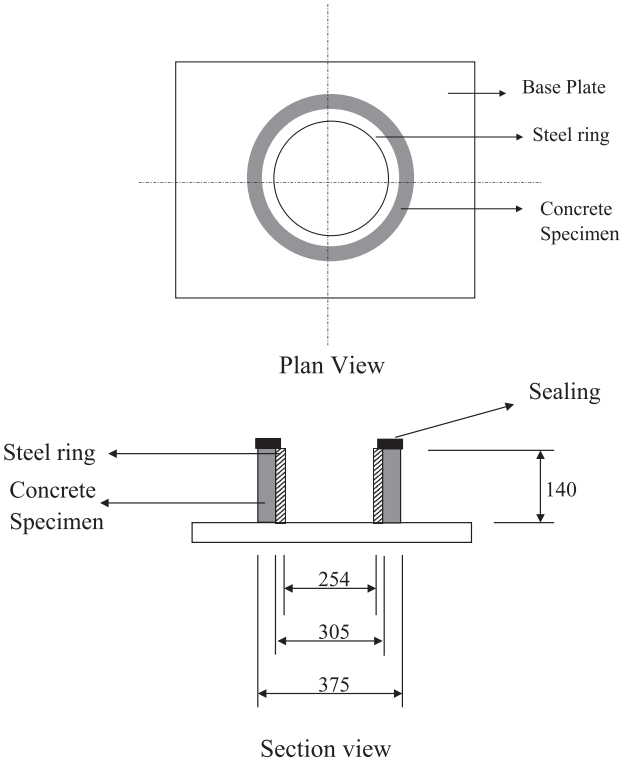

Fig. 1. Restrained shrinkage ring specimen (in mm).

radial stress was 20% of the maximum hoop stress. Thus, it can be assumed that the concrete annulus was essentially subjected to a uniform, uniaxial tensile stress when it was internally restrained by the steel ring. In addition, the width of the specimen (140 mm) was four times its thickness (35 mm), so that a uniform shrinkage along the width of the specimen can be assumed [13,15–17].

2.4. Curing of the specimens

Free and restrained shrinkage specimens were cured for 24 h at 20 °C and 100% relative humidity and were then demoulded. After the outer steel ring had been stripped off, the top surface of the concrete ring was sealed off using silicon rubber, so that the drying would be allowed only from the outer circumferential surface. After that, the specimens were exposed to drying in a humidity cabinet at 23 ± 2 °C and 50 ± 5% relative humidity, as per ASTM C157-75 [19] for about 50 days. All the other test specimens were first maintained under plastic sheets for 24 h and were then demoulded. Specimens for creep, compressive strength, split-tensile strength, and modulus of rupture were water-cured for 28 days after demoulding.

2.5. Measurements and testing

Free shrinkage measurements were performed according to ASTM C157-75 [19]. The length change was measured by means of a dial gage extensometer with a 200-mm gage length. Measurements were carried out every 24 h for the first 3 weeks and then 3 times a week. At the same time, weight loss measurements were also made on the same specimens. To measure the crack widths on ring specimens, a special microscope setup was used as proposed in Refs. [13,15–17]. The microscope was attached to an adjustable scaled locator connected to a vertical bar passing through the inner steel ring and fixed at the center of the base plate in such a way that it enabled the microscope to move around the specimen. A locator was connected to the horizontal bar, permitting up-and-down movement, so that the whole circumferential surface of the specimen could be observed with the microscope. The crack widths reported herein were the average of three measurements: one at the center of the ring and the other two at the centers of the top and bottom halves of the ring. The surface of the specimens was examined for new cracks, and the measurement of the existing crack widths were performed every 24 h during the first 7 days after cracking, and then every 48 h. Free shrinkage strains and the crack widths given here are the average of four prisms and two ring specimens, respectively.

Creep tests were performed at the age of 28 days according to ASTM C512 [20]. Two specimens were loaded in series up to 35% of the compressive strength of the concrete obtained at the same age. The specimens under the sustained load were maintained in the curing room at 23 ± 2 °C and 60 ± 5% relative humidity for 90 days. Length change of the creep specimens was measured on two opposite sides by a dial gage extensometer with a 50-mm gage length. An unloaded specimen accompanied the loaded ones to monitor the shrinkage deformation. Thus, the creep strain was obtained as the total strain less the shrinkage and elastic strains.

Compression, static elastic modulus, and splitting tensile tests were carried out at the 28th days according to the relevant ASTM standards.

Fig. 2. Photographic view of a cracked ring specimen (M6).

3. Experimental results and discussion

3.1. Fresh concrete properties

Concretes produced had slumps within 200 ± 20 mm which was achieved by using varying amounts of a high-range water-reducing admixture. The concretes were of cohesive and sticky consistency. Fresh density of the concretes ranged from 2170 to 1950 kg/m^3 (Table 3). The fresh densities seem to be slightly high for LWCs. This might be attributed to three reasons. First, w/cm was low, and the cement content was high. Second, specific gravity of the fly ash was rather high resulting in artificial aggregates having a specific gravity of 1.78, which was slightly large for use in LWC. Finally, the main reason was the use of natural sand as fine aggregate, which caused all the concretes to exceed the ACI limitation as far as the density of the concrete was concerned. However, similar results were reported in previous studies [2–4]. Air contents of the mixtures were determined through calculating the actual compositions, and the values were in the range of 1.5–2.5%.

3.2. Compressive strength and static elastic modulus

A summary of the test results regarding the compressive strength and modulus of elasticity of the LWCs are given in Table 4, and comparisons were made through the table and Figs. 3 and 4. Fig. 3 shows the variation of compressive strength with the w/cm, the use of silica fume, and the lightweight coarse aggregate volume concentration. The compressive strengths ranging from 20.8 to 47.3 MPa for all mixtures satisfied the lower limit (17.2 MPa) to be used for structural purposes [21]. The concrete mixture containing silica fume, with 0.32 w/cm and lightweight coarse aggregate volume concentration of 30%, had the highest compressive strength. Fig. 3 also indicates that when the amount of lightweight aggregate increased, the compressive strength gradually decreased because the artificial fly ash aggregates were weaker than the matrix. A decrease in the w/cm from 0.55 to 0.35 resulted in a substantial increase in the compressive strength by 86%, 60%, and 40% for the concretes with 30%, 45%, and 60% coarse aggregate volume, respectively, and containing no silica fume. However, this increase was approximately 50% for all concretes with silica fume. For the concretes with weaker matrices, namely, M7, M8, and M9, the effect of the lightweight aggregate content diminished significantly. The addition of silica fume enhanced the compressive strength for all concretes due to subsequent decrease in w/cm. However, this beneficial effect was less for the concretes of low w/cm inasmuch as the further improvement of the matrix did not necessarily mean higher compressive strength for concrete due to the earlier failure of the lightweight coarse aggregate particles. With the use of silica fume and thus decreasing the w/cm from 0.35 to 0.32 and from 0.55 to 0.50 for both mixtures, the increase in the compressive strength was 18%, 6%, and 29%, and 41%, 9%, and 18% at 30%, 45%, and 60% aggregate volume concentrations, respectively. It was seen that silica fume was less effective at medium concentrations of the lightweight coarse aggregate.

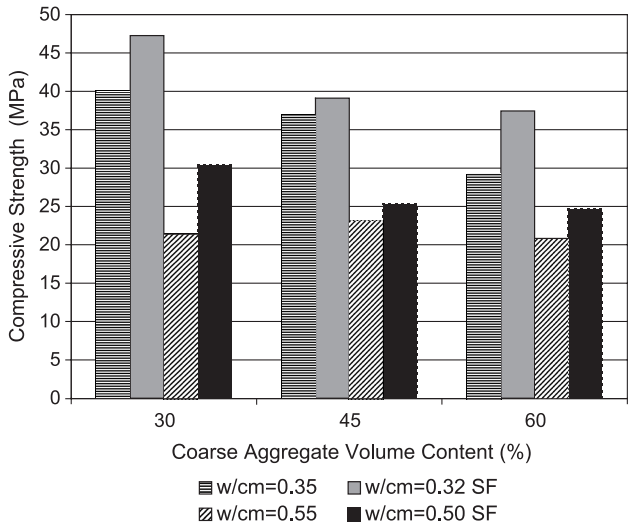

Fig. 3. Variation in compressive strength for different concrete mixes.

Table 4
Test results of compressive and tensile strengths, and static elastic modulus

Mix no.	Compressive strength (MPa)	Splitting-tensile strength (MPa)	Static elastic modulus (GPa)
M1	40.1	3.22	22.44
M2	36.9	2.86	20.05
M3	29.1	2.58	18.19
M4	47.3	3.94	24.43
M5	39.1	3.17	23.19
M6	37.5	2.58	21.81
M7	21.5	2.35	19.08
M8	23.2	2.16	17.01
M9	20.8	1.86	14.22
M10	30.4	2.67	21.96
M11	25.3	2.35	18.32
M12	24.6	2.12	16.48

Static elastic moduli of the concretes also decreased gradually with increasing lightweight coarse aggregate content (Fig. 4). Concretes with lower w/cm had higher modulus of elasticity. Silica fume concretes had greater elastic moduli by approximately 9%, 15%, and 20% for low w/cm, and 16%, 6%, and 16% for higher w/cm. It was observed that silica fume was less effective at 45% lightweight aggregate concentration as for the compressive strength. Elastic moduli for the concrete mixtures varied from 14.2 to 24.4 GPa. Moreover, Table 5 shows the comparison of the experimental values of the modulus of elasticity with those predicted by the various equations given in ACI 318 [22], Norwegian Concrete Code "NS

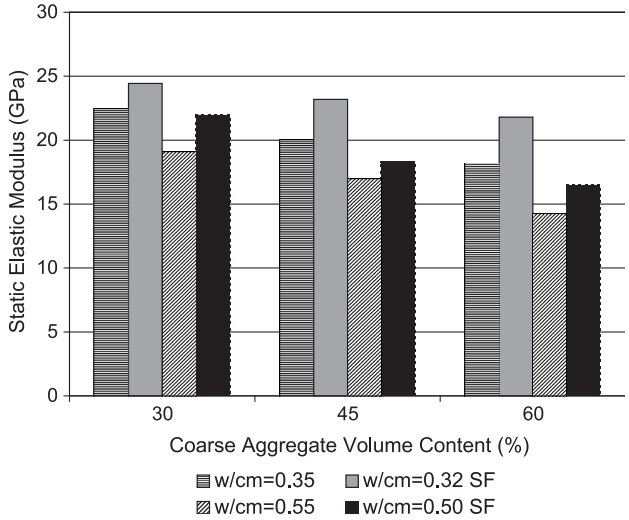

Fig. 4. Variation in static elastic modulus for different concrete mixes.

3473" [23], British standard "BS 8110" [24], and the equation given by Slate et al. [25] as specified below.

$$\text{ACI 318: } E_c = 0.043 w^{1.5}\sqrt{f_c} \quad (1)$$

$$\text{NS 3473: } E_c = 9500 f_{cck}^{0.3}\left(\frac{w}{2400}\right)^{1.5} \quad (2)$$

$$\text{BS 8118: } E_c = 0.0017 w^2 f^{0.3} \quad (3)$$

$$\text{Slate et al.: } E_c = (3320\sqrt{f_c} + 6895)\left(\frac{w}{2320}\right)^{1.5} \quad (4)$$

where E_c is the modulus of elasticity of the concrete (MPa); w is the air dried density of the concrete (kg/m^3); f_{cck} is the cylinder compressive strength measured on 100 × 200-mm specimens (MPa); f_c is the cylinder compressive strength measured on 150 × 300-mm specimens (MPa); f is the 150-mm cube compressive strength (MPa).

To make use of the above equations, 100-mm cube compressive strengths were converted to 100 × 200- and 150 × 300-mm cylinder strengths, and 150-mm cube compressive strengths in the same way by multiplying by a factor of 0.9 [26]. Measured fresh densities were used in the above equations. As it is seen from Table 5, the predicted values of static elastic moduli agreed well with the test results for all equations.

Table 5
Comparison of observed and predicted elastic moduli

Mixture no.	Observed values of E (GPa)	Predicted values of E (GPa)			
		ACI 318	NS 3473	BS 8110	Slate et al. [25]
M1	22.44	24.60	23.94	23.54	23.24
M2	20.05	22.50	22.26	21.53	21.49
M3	18.19	18.78	19.47	18.45	18.56
M4	24.43	26.45	24.90	24.39	24.45
M5	23.19	22.90	22.39	21.58	21.70
M6	21.81	21.45	21.15	20.09	20.44
M7	19.08	17.09	18.84	18.20	17.73
M8	17.01	16.98	18.42	17.52	17.38
M9	14.22	15.22	16.89	15.78	15.87
M10	21.96	20.30	20.87	20.15	19.93
M11	18.32	17.63	18.81	17.87	17.81
M12	16.48	16.44	17.63	16.43	16.67

3.3. Split-tensile strength

Table 4 also presents the indirect tensile strength of concretes measured through splitting tests which are also shown in Fig. 5. The split-tensile strengths exhibited a gradual decrease as the volume ratio of the lightweight coarse aggregate increased from 30% to 60%. This reduction was most dramatic for the silica fume concretes with w/cm of 0.32. Decreasing the w/cm and the use of silica fume enhanced the splitting tensile strengths. The concretes with silica fume had splitting tensile strengths which were about 12% greater than those without silica fume at high w/cm. The effect of silica fume was highest at low lightweight coarse aggregate concentration at low w/cm but diminished to null with increase in the coarse aggregate content. The split-tensile strength ranged from 1.86 to 3.94 MPa when the compressive strength increased from 20.8 to 47.3 MPa. The ratio of the former to the latter ranged from 7.8% to 9.7% for all the concrete mixtures, where the addition of silica fume caused a slight decrease in this ratio, inasmuch as the enhancement due to silica fume and thus reduced w/cm was higher in the compressive strength. Chang and Shieh [2] gave this ratio as 9% to 11% for the concretes made with cold-bonded aggregates. The ratio was about 7% for a concrete having a compressive strength of 51 MPa and made with sintered fly ash aggregates [11]. Zhang and Gjorv [26], and Khaloo and Kim [27] revealed that for compressive strength ranging from 50 to 100 MPa, this ratio was approximately 5%. In addition, they found a relation be-

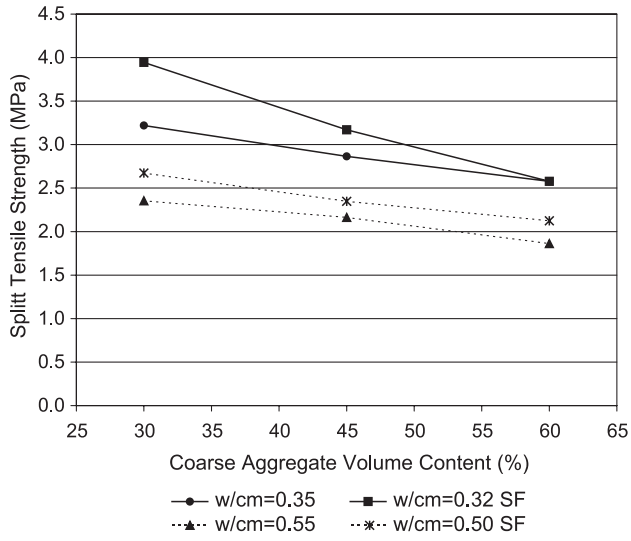

Fig. 5. Splitting tensile strength of different concrete mixes.

tween splitting tensile and compressive strength for compressive strength ranging from 57 to 102 MPa, as given in Eq. 5 [26]:

$$f_{ct} = 0.23\sqrt[3]{f_{ck}^2} \quad (5)$$

The relation obtained in this study is given in Eq. 6 for compressive strength between 20.8 and 47.3 MPa:

$$f_{ct} = 0.27\sqrt[3]{f_{ck}^2} \quad (6)$$

In the above equations, f_{ct} is the splitting tensile strength measured on 100 × 200-mm cylinders, and f_{ck} is the 100-mm cube compressive strength in MPa, respectively.

3.4. Free shrinkage and weight loss

Free shrinkage tests can provide necessary information on how the drying shrinkage stresses develop, although they cannot offer sufficient information on the behavior of concrete structures [13].

Variation of drying shrinkage and weight loss with time for the concretes studied are shown in Figs. 6 and 7, respectively. The final shrinkage and weight loss values obtained after 50 days of drying are given in Table 6. As it is seen from Fig. 6, the free shrinkage strains were comparable at early ages of the drying period. However, a clear distinction was observed for different concrete mixtures after about a week. Concretes of higher lightweight coarse aggregate content demonstrated higher shrinkage for all w/cm, but this effect was more indicative for the higher w/cm. Although the lightweight coarse aggregate particles provided water into the drying matrix at the very early ages and thus extended the cracking time by reducing the autogenous shrinkage, higher unit water content resulted in higher shrinkage values at later ages. Concretes with silica fume shrunk more than the plain concrete, especially in the case of higher w/cm inasmuch as the addition of silica fume increased the total cementitious material content and resulted in finer pore structure and proportionally higher free shrinkage [13,28]. Maximum shrinkage strains at 50 days were about five and 25% greater for low and high w/cm, respectively, at all coarse aggregate contents. Moreover, low-w/cm concretes without silica fume experienced higher shrinkage strains, but the addition of silica fume into the concretes substantially reduced the difference due to increase in w/cm. The shrinkage strains increased 24%, 23%, and 19% for the increasing coarse aggregate contents as the w/cm was decreased from 0.55 to 0.35, whereas this difference was only 4% in the case of the silica fume concretes.

Table 6
Final values for drying shrinkage test results at 50 days

Mix	Maximum free shrinkage (microstrain)	Maximum weight loss (g)	Average cracking age (days)	Maximum crack width (mm)
M1	1410	98.4	7	2.96
M2	1428	108.6	7	3.02
M3	1506	135.7	8	3.2
M4	1475	92.0	6	3.4
M5	–	–	–	–
M6	1576	115.3	6	4.52
M7	1132	128.0	11	2.17
M8	1160	137.0	11	2.2
M9	1260	168.0	12	2.32
M10	1412	120.4	8	2.61
M11	–	–	–	–
M12	1564	163.8	10	3.25

The weight loss with respect to time for all concretes are shown in Fig. 7. The weight losses for different concretes were similar at early ages. However, clear distinctions could be observed at 10 days onwards. For the same w/cm, higher amount of coarse aggregate gave rise to greater water loss inasmuch as the lightweight aggregates were used in SSD condition, which in turn increased the unit water content. This behavior also explained the higher free shrinkage for these concretes. However, for the concretes without silica fume the free shrinkage strains were higher for the low w/

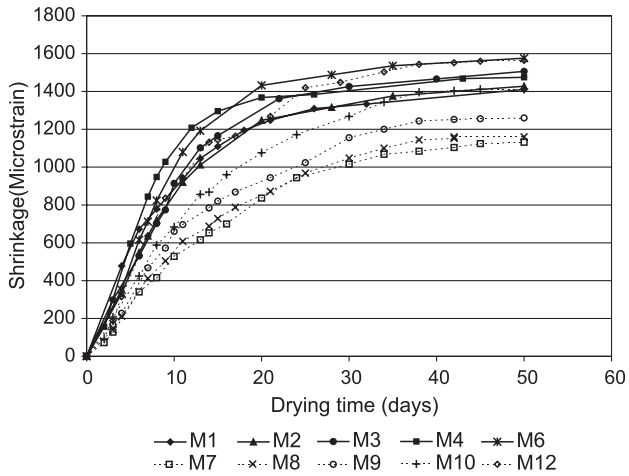

Fig. 6. Free shrinkage of concretes.

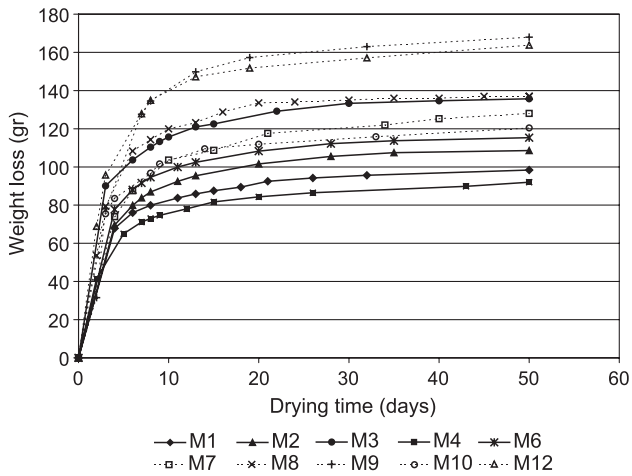

Fig. 7. Weight loss of concretes.

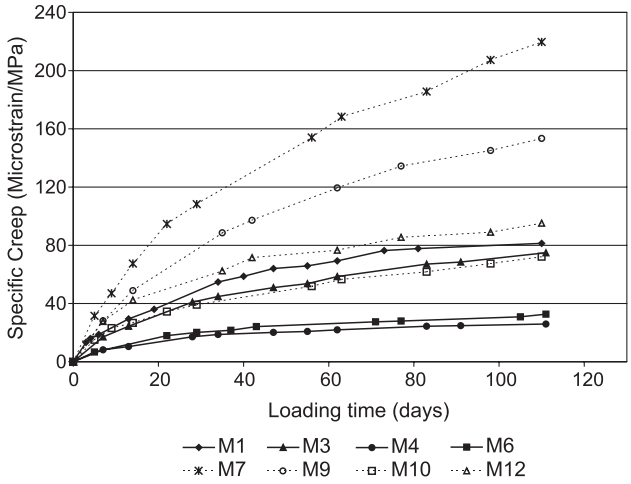

Fig. 8. Specific creep of concretes.

cm despite the fact that the corresponding weight losses were smaller than those of high w/cm. Similar results were obtained for the silica fume concretes. This behavior is attributed to the fact that free shrinkage is related to other factors in addition to weight loss [13]. One possible explanation may be that concrete with higher amount of cementitious materials has finer pore structure that may proportionally increase free shrinkage [28].

3.5. Creep

Creep test results are expressed in specific creep and are shown in Fig. 8. Concretes were loaded at 35% of the compressive strength obtained at 28 days, resulting in different absolute stress levels in creep tests. It is observed from the figure that the specific creep significantly decreased with using silica fume for all concretes irrespective of the lightweight coarse aggregate content. This is because the concrete with silica fume had higher compressive strength resulting from the increased total cementitious material content as well as filling and pozzolanic effect of silica fume. However, the reduction in the final creep by the inclusion of silica fume was more pronounced for the concretes containing less amount of lightweight aggregate. This behavior is particularly important inasmuch as the silica fume concretes cracked earlier than the companion plain concretes. Moreover, the crack width was larger, and the rate of crack development was faster for silica fume concretes. Similar behavior was observed in NWC regarding the effect of silica fume [13,29]. Fig. 8 also revealed that the specific creep was remarkably greater (approximately triple) for the high-w/cm concretes. Unlike the free shrinkage, the specific creep decreased with the increase in the lightweight coarse aggregate content. The specific creep at 90 days dropped from 80 to 70 (μs/MPa) and from 220 to 150 (μs/MPa) for the concretes without silica fume when the coarse aggregate volume ratio increased from 30% to 60%. The opposite of this, however, was observed for the silica fume concretes. Although the lightweight coarse aggregate particles were weaker than the mortar phase, the decrease in the sand content induced this behavior [8].

3.6. Restrained shrinkage cracking

Shrinkage cracking age and the maximum crack width of the LWCs are given in Table 6, and the crack development within time for different concretes are shown in Fig. 9. At low w/cm, plain concretes cracked at 7 and 8 days depending on the coarse aggregate volume ratio, whereas the cracking occurred at 6 days for the silica fume concretes. At high w/cm, on the other hand, the cracks were first seen at 11 and 12 days for plain concretes and at 8 and 10 days for the concretes with silica fume. Despite the fact that the concretes with 60% coarse aggregate volume ratio had higher free shrinkage, lower tensile strength and specific creep, the cracking time was extended 1 or 2 days than the concretes with 30% or 45% lightweight aggregate. This might be attributed to the fact that the lightweight coarse aggregate particles in SSD condition supplied water into the concrete during early ages of drying period, which in turn reduced the self-desiccation [30]. Furthermore, the lower elastic moduli of these concretes helped in extending the cracking time. However, this was not observed in the silica fume concretes with 0.32 w/cm. As it is seen from Table 6 and Fig. 9, shrinkage cracking was observed at earlier ages for silica fume concretes, especially in those of 0.50 w/cm. In addition, the crack opening was faster in the first few days, and the maximum crack widths at 50 days were 15% to 40% higher depending on the coarse aggregate content for both 0.32 and 0.50 w/cm. This behavior resulted from the combined effect of higher free shrinkage, lower specific creep, and higher elastic modulus for silica fume concretes, although their tensile strengths were greater. Like silica fume, lower w/cm accompanied by higher cement content resulted in early cracking of the concretes. The cracking was observed 4 days prior to those at 0.55 w/cm. Furthermore,

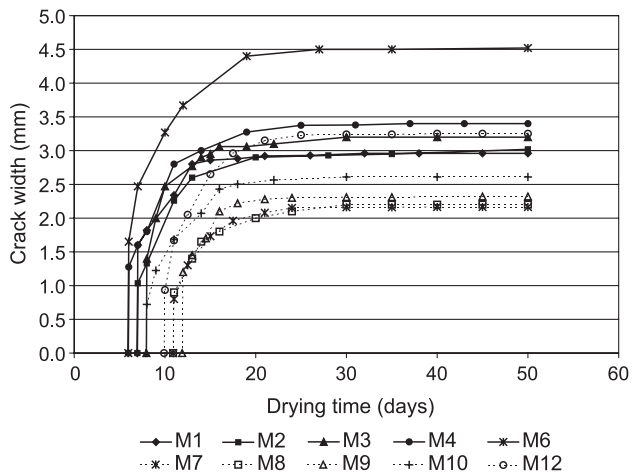

Fig. 9. Restrained shrinkage cracking of concretes.

the crack width at 50 days was 35% larger, and the crack development was faster at all lightweight coarse aggregate contents. Fig. 9 also indicates that the crack opening stabilized after about 15 days in all cases.

Shrinkage cracking performance of the LWC was significantly poorer than NWC when Tables 1 and 6 are compared. Although the free shrinkage values were almost double, the crack opening was much larger reaching to five times, for LWC in comparison to NWC. The cracking time of the former, on the other hand, was longer than the latter inasmuch as the lightweight aggregate behaved as a water reservoir by providing water into the concrete during the early ages of the drying, thus extending the cracking time.

4. Conclusions

Based on the results obtained from this study, the following conclusions may be drawn:

1. Structural LWCs were produced with cold-bonded fly ash aggregates. The compressive strength ranged from 20.8 to 47.3 MPa. However, higher coarse aggregate volume ratio resulted in a gradual decrease in the compressive strength. This negative effect was less pronounced at 0.55 w/cm. Addition of silica fume and thus increasing the total cementitious material content increased the compressive strength at some level, especially at high w/cm ratio.
2. Static elastic modulus ranged from 14.2 to 24.4 GPa, decreasing with higher lightweight coarse aggregate concentration. The experimental values were compared with those predicted by the equations given by ACI 318, NS 3473, BS 8110, and Slate et al. [25]. The predicted values agreed well with the test results. The prediction was generally within $\pm$ 12%.
3. Split-tensile strength of the concretes also decreased with the lightweight coarse aggregate content. The reduction in split-tensile strength was more marked for the concretes of low w/cm and/or silica fume. The ratio of split-tensile strength to corresponding cube compressive strength were 8% and 10% at low and high w/cm, respectively.
4. Shrinkage strains at 50 days were higher for the concretes incorporating lightweight aggregates at higher quantities. This might be due to the excess water in the mixture supplied by the saturated lightweight coarse aggregates. Although the plain concretes with low w/cm had higher shrinkage than high w/cm concretes, the addition of silica fume reduced the difference substantially.
5. For the same w/cm, concretes with higher lightweight coarse aggregate content lost more water. This may explain the higher shrinkage strain for these concretes. However, the weight loss were higher at 0.55 w/cm despite the corresponding shrinkage strain being smaller. Similar results were observed for silica fume concretes.
6. Specific creep reduced significantly for the silica fume concretes at both low and high w/cm. Concretes without silica fume at low w/cm showed lower creep values. In addition, concretes containing higher lightweight coarse aggregate content had lower creep strain at all w/cm.
7. Shrinkage cracking was observed at about 7 and 11 days for the plain concretes at 0.35 and 0.55 w/cm, respectively. With the addition of silica fume, the cracking took place earlier. The combined action of higher free shrinkage, higher elastic modulus, and lower specific creep resulted in earlier cracking of the plain concretes at 0.35 w/cm and all silica fume concretes at both w/cm of 0.32 and 0.50 in spite of their higher tensile strengths. The concretes with 60% lightweight coarse aggregate volume ratio cracked 1 or 2 days after their counterparts with less lightweight coarse aggregate content. This might be due to the reduction in self-desiccation of these concretes at early ages inasmuch as the lightweight coarse aggregate particles might supply water as the concrete dried.
8. Compared to the NWC as reported in the literature, shrinkage cracking performance of LWC was much poorer.

References

[1] M.H. Zhang, O.E. Gjorv, Characteristics of lightweight aggregates for high strength concrete, ACI Mater. J. 88 (2) (1991) 150–158.
[2] T.P. Chang, M.M. Shieh, Fracture properties of lightweight concrete, Cem. Concr. Res. 26 (2) (1996) 181–188.
[3] C.C. Yang, Approximate elastic moduli of lightweight aggregate, Cem. Concr. Res. 27 (7) (1997) 1021–1030.
[4] A. Mor, Steel–concrete bond in high-strength lightweight concrete, ACI Mater. J. 89 (1) (1992) 76–82.
[5] N. Haque, H. Al-Khaiyat, Strength and durability of lightweight concrete in hot marine exposure conditions, Mater. Struct. 32 (1999) 533–538.
[6] H. Al-Khaiyat, N. Haque, Strength and durability of lightweight and normal weight concrete, J. Mater. Civ. Eng. 11 (3) (1999) 231–235.
[7] O. Kayali, M.N. Haque, B. Zhu, Drying shrinkage of fibre-reinforced lightweight aggregate concrete containing fly ash, Cem. Concr. Res. 29 (1999) 1835–1840.
[8] A.M. Neville, Properties of Concrete, 4th ed., Longman, London, 1995.
[9] U. Nielsen, P.C. Aitcin, Properties of high-strength concrete containing light, normal, and heavyweight aggregate, Cem., Concr. Aggreg. 14 (1) (1992) 8–12.
[10] J.B. Newman, Properties of structural lightweight aggregate concrete, in: J.L. Clarke (Ed.), Structural Lightweight Aggregate Concrete, Chapman & Hall, London, 1993, pp. 19–44.
[11] H. Al-Khaiyat, M.N. Hague, Effect of initial curing on early strength and physical properties of a lightweight concrete, Cem. Concr. Res. 28 (6) (1998) 859–866.
[12] S.A. Altoubat, D.A. Lange, Creep, shrinkage, and cracking of restrained concrete at early age, ACI Mater. J. 98 (4) (2001) 323–331.
[13] K. Wiegrink, S.M. Marikunte, S.P. Shah, Shrinkage cracking of high-strength concrete, ACI Mater. J. 93 (5) (1996) 409–415.
[14] N. Banthia, C. Yan, Shrinkage cracking in polyolefin fiber-reinforced concrete, ACI Mater. J. 97 (4) (2000) 422–427.
[15] M. Grzybowski, S.P. Shah, Shrinkage cracking of fiber reinforced concrete, ACI Mater. J. 87 (2) (1990) 138–148.
[16] S.P. Shah, M.E. Karaguler, M. Sarigaphuti, Effects of shrinkage-re-

ducing admixtures on restrained shrinkage cracking of concrete, ACI Mater. J. 89 (3) (1992) 289–295.
[17] M. Sarigaphuti, S.P. Shah, K.D. Vinson, Shrinkage cracking and durability characteristics of cellulose fiber reinforced concrete, ACI Mater. J. 90 (4) (1993) 309–318.
[18] B. Malmberg, A. Skarendahl, Method of Studying the Cracking of Fibre Concrete under Restrained Shrinkage, Int. RILEM Symp. on Testing and Test Methods of Fibre Cement Composites, The Construction Press, Lancaster, 1978, pp. 173–179.
[19] ASTM C157, Standard Test Method for Length Change of Hardened Hydraulic-Cement Mortar and Concrete, Annual Book of ASTM Standards, V. 04-02, 1997, pp. 96–101.
[20] ASTM C512, Standard Test Method for Creep of Concrete in Compression, Annual Book of ASTM Standards, V. 04-02, 1997, pp. 267–270.
[21] ACI Committee 213, Guide for Structural Lightweight Aggregate Concrete, (ACI 213R-87), American Concrete Institute, Farmington Hills, MI, 1987.
[22] ACI Committee 318, Building code requirements for reinforced concrete (ACI 318-95), American Concrete Institute, Farmington Hills, MI, 1995.
[23] NS 3473, Norwegian Concrete Code, Norwegian Concrete Association, Oslo, 1992 (in Norwegian).
[24] British Standard BS 8110: Part 2. British Standard Institution, 1985.
[25] F.O. Slate, A.H. Nilson, S. Martinez, Mechanical properties of high strength lightweight concrete, Proc. - Am. Concr. Inst. 83 (4) (1986) 606–613.
[26] M.H. Zhang, O.E. Gjorv, Mechanical properties of high strength lightweight concrete, ACI Mater. J. 88 (3) (1991) 240–247.
[27] A.R. Khaloo, N. Kim, Effect of curing condition on strength and elastic modulus of lightweight high-strength concrete, ACI Mater. J. 96 (4) (1999) 485–490.
[28] M. Regourd, Microstructure of high strength cement based systems, Materials Research Society Proceedings Series V. 2, Materials Research Society, Warrendale, PA, 1985, pp. 3–17.
[29] L. Jianyong, Y. Yan, A study on creep and drying shrinkage of high performance concrete, Cem. Concr. Res. 31 (2001) 1203–1206.
[30] K. Kohno, T. Okamoto, Y. Isikawa, T. Sibata, H. Mori, Effects of artificial lightweight aggregate on autogenous shrinkage of concrete, Cem. Concr. Res. 29 (1999) 611–614.